Direct vs redistributed fluorescence of supercooled molecules: The onset of intramolecular vibrational redistribution

Shaul Mukamel[a)]
Department of Chemistry, University of Rochester, Rochester, New York 14627
and Laboratoire de Photophysique Moleculaire, University of Paris sud Orsay, 91405 France

(Received 17 September 1984; accepted 10 December 1984)

The observability and relative yield of distinct "direct" and "redistributed" components in the fluorescence of supercooled molecules is analyzed. The static and dynamic effects of anharmonicities underlying the redistributed component and their implication for experiments which are both time and frequency resolved, are specified. Analysis of the recent picosecond beam studies of Felker and Zewail in Anthracene shows evidence for a selective anharmonic coupling scheme in which the doorway state is coupled to a few harmonic states which are sequentially coupled to the other harmonic states.

I. INTRODUCTION

Frequency-resolved fluorescence spectra of ultracold polyatomic molecules in supersonic beams provide a useful means for studying intramolecular vibrational dynamics. Some general features characterize the variety of molecules studied, such as benzene derivatives, large aromatic molecules, and porphyrins.[1-13] The absorption (excitation) spectra are discrete, consisting of progressions of a few well-resolved optically active modes. The dispersed fluorescence spectra arising from excitation to the ground vibronic level (0–0 band) are similar in character to the absorption. However, at higher levels of excitation, the fluorescence typically consists of a discrete range of isolated lines followed by a complicated continuous spectrum which starts at some threshold. It is clear that the appearance of the latter complex spectrum is a signature of the molecular anharmonicities. Spectra of harmonic molecules will show only the optically active modes whose number is relatively small (e.g., 6 for alkyl benzenes).[14] The broad continuum arises from emission from the other modes which are accessible only via the anharmonicities. The fundamental issue which remains unanswered by the frequency-resolved spectra is whether the anharmonicities enter the picture merely statically (via state mixing) or via a dynamical process of intramolecular vibrational redistribution (IVR). A discussion of that point was made recently[2,4,14,15] but the available frequency-resolved spectra do not provide an answer and are inconclusive.[3,14,15] Parmenter and co-workers have used chemical timing (i.e., collisional deactivation) to obtain the short-time emission spectra.[2] Their results show an evidence for IVR processes which occur on picosecond time scales. Felker and Zewail[16] have recently successfully conducted picosecond studies of anthracene in a beam and obtained the time- and frequency-resolved spectra. These remarkable experiments demonstrate clearly how spectra which are both time- and frequency resolved may carry a significant dynamical information even in congested spectral regions with a high density of states, whereby ordinary fluorescence, which is only frequency resolved, may be very complex. These experiments[16] allow us to discuss with confidence the dynamical effects of anharmonicities in polyatomics. The purpose of the present note is to clarify the connection between time-resolved and frequency-resolved experiments and to provide simple criteria for classifying the various possible cases and their information content. Particular attention is given to the relative yield of the direct and the redistributed components and its dependence on detuning and on time. Our analysis is an extension of earlier treatments developed for radiationless transitions and IVR processes.[15-17]

II. THE EXPERIMENTAL OBSERVABLES

Consider the following molecular level scheme (Fig. 1): The molecule is initially at zero temperature in the ground vibronic state $|g\rangle$. It is excited by absorbing an ω_L photon to a manifold of vibronic states belonging to an excited electronic state. The states $|s\rangle$ and $\{|l\rangle\}$ are harmonic zero-order states coupled by the anharmonic interactions V_{sl}. We further assume that only one zero-order state, the doorway state $|s\rangle$, carries oscillator strength from $|g\rangle$. Both $|s\rangle$ and $\{|l\rangle\}$ can emit an ω_s photon and end up in the manifold $|g'\rangle$ of vibronic eigenstates of the ground electronic state. In this section we shall not go any further into the nature of the $|s\rangle$ and $|l\rangle$ states. It will be shown in the next section that the harmonic basis set, by virtue of its selection rules, provides a simple description of the distinction between the "direct" and "redistributed" parts of the fluorescence spectrum. For the present discussion it will be sufficient to consider the exact molecular eigenstates $|j\rangle$ which diagonalize the electronically excited molecular Hamiltonian H, that is,

$$|j\rangle = \alpha_j|s\rangle + \sum_l \beta_{jl}|l\rangle, \tag{1a}$$

with

$$H|j\rangle = \left(E_j - \frac{i}{2}\Gamma_j\right)|j\rangle. \tag{1b}$$

[a)] Alfred P. Sloan Fellow, Camille and Henry Dreyfus Teacher–Scholar.

 0021-9606/85/072867-10$02.10

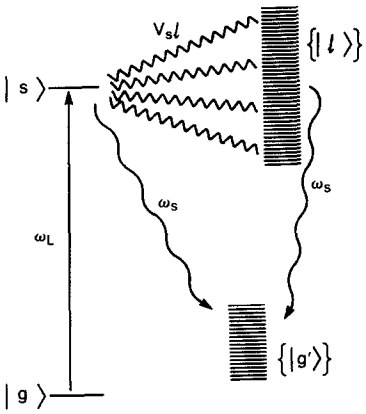

FIG. 1. The level coupling scheme. $|s\rangle$ is the doorway harmonic state coupled radiatively to $|g\rangle$ and via the anharmonicities V_{sl} to the $\{|l\rangle\}$ manifold. $\{|g'\rangle\}$ are vibronic states belonging to the ground electronic state.

Here α_j and β_{jl} are the anharmonic mixing coefficients of these states, and E_j and Γ_j are the energy and the width of the $|j\rangle$ state. Note that if Γ_j is purely radiative, then for our model system it will be independent of j, since $|s\rangle$ and $\{|l\rangle\}$ have the same radiative width. This model was treated in detail in the context of radiationless transitions whereby $|s\rangle$ and $\{|l\rangle\}$ belong to different electronic states[17–20] and the coupling V_{sl} is either vibronic or spin orbit. In the present article, we consider intrastate anharmonic coupling and $|s\rangle$ and $\{|l\rangle\}$ to belong to the same electronic state. We shall now introduce the various experimental observables in time- and frequency-resolved fluorescence spectra,[15,17b] which form the basis for our discussion in the next section.

A. The absorption spectrum

This is the simplest observable usually measured in excitation spectra although direct absorption measurements are now feasible.[21] It is given by the simple golden rule expression:

$$I_a(\omega_L) = \sum_j |\mu_{jg}|^2 \delta(\omega_{gj} + \omega_L). \tag{2}$$

Here $\omega_{gj} \equiv E_g - E_j$ and μ_{jg} is the transition dipole matrix element. The δ function should be understood as a narrow Lorentzian whose FWHM is $\Gamma_j + \Gamma_g$.

B. Frequency-resolved fluorescence

In an ideal steady state experiment with a weak monochromatic excitation at frequency ω_L the molecule attains a steady state whereby the vibronic wave function becomes

$$|\psi\rangle = |g\rangle + |\psi_e\rangle, \tag{3}$$

with $|\psi_e\rangle$ being the excited state part given by (to first order in μ)

$$|\psi_e\rangle = \sum_j \mu_{jg} \frac{1}{\omega_{gj} + \omega_L + (i/2)\Gamma_j} |j\rangle. \tag{4}$$

The weight of $|j\rangle$ is governed by its dipole coupling μ_{jg} with the initial state, and by a resonant denominator which selects states with $\omega_{jg} \cong \omega_L$.

The photon emission rate is then again given by the Fermi "golden rule":

$$I(\omega_L, \omega_s) = \sum_{g'} |\langle g'|\mu|\psi_e\rangle|^2 \delta(\omega_{g'g} - \omega_L + \omega_s)$$
$$= \sum_{g'} \left| \sum_j \frac{\mu_{g'j}\mu_{jg}}{\omega_{gj} + \omega_L + (i/2)\Gamma_j} \right|^2 \times \delta(\omega_{g'g} - \omega_L + \omega_s). \tag{5}$$

C. Pulsed excitation with time and spectrally resolved detection

We shall turn now to more detailed experimental observables involving a *pulsed excitation* followed by *a time- and frequency-resolved detection.* We assume an excitation pulse whose electric field is given by

$$E_L(t) = \phi(t)\exp(-i\omega_L t) + \text{c.c.} \tag{6}$$

Here $\phi(t)$ is the pulse envelope function and

$$J(t) = |\phi(t)|^2 \tag{7a}$$

is the time-dependent pulse intensity. The power spectrum of the pulse is

$$J(\omega) = |\phi(\omega)|^2, \tag{7b}$$

where

$$\phi(\omega) = \int d\tau \exp[i(\omega - \omega_L)\tau]\phi(\tau). \tag{7c}$$

The most detailed observable[22] in a time-resolved experiment is the rate of emission of an ω_s photon at time t to a final molecular state $|g'\rangle$. This can be calculated using second-order perturbation theory, resulting in[17b]

$$I_{g'}(\omega_L, \omega_s, t) = \frac{d}{dt}|C_{g'g}(t)|^2, \tag{8}$$

with the total emission rate of ω_s photons at time t given by

$$I(\omega_L, \omega_s, t) = \sum_{g'} I_{g'}(\omega_L, \omega_s, t). \tag{8a}$$

Here

$$C_{g'g}(t) = \int_{-\infty}^{t} d\tau_1 \exp[-i(\omega_s + E_{g'})(t - \tau_1)] \times \langle N_{g'}|\psi_e(\tau_1)\rangle, \tag{9}$$

with

$$\langle N_{g'}|\psi_e(\tau_1)\rangle = \int_{-\infty}^{\tau_1} d\tau_2 \times \langle N_{g'}|N_g(\tau_1 - \tau_2)\rangle\phi(\tau_2)\exp[-i(\omega_L + E_g)\tau_2]. \tag{10}$$

Here $|N_g\rangle$ and $|N_{g'}\rangle$ are the *doorway states* associated with the states $|g\rangle$ and $|g'\rangle$, respectively. They are (unnormalized) wave packets of excited vibronic states[15,17b]

$$|N_g\rangle \equiv \mu|g\rangle = \sum_j \mu_{jg}|j\rangle \tag{11a}$$

and

$$|N_{g'}\rangle \equiv \mu|g'\rangle = \sum_j \mu_{jg'}|j\rangle. \tag{11b}$$

The quantity $\langle N_{g'}|N_g(\tau_1 - \tau_2)\rangle$ is the overlap of the $|N_g\rangle$ doorway state propagated for time $\tau_1 - \tau_2$ with $|N_{g'}\rangle$ and is given by

$$\langle N_{g'}|N_g(\tau_1 - \tau_2)\rangle \equiv \langle N_{g'}|\exp[-iH(\tau_1 - \tau_2)]|N_g\rangle = \sum_j \mu_{jg}\mu_{g'j} \times \exp[-iE_j(\tau_1 - \tau_2) - \tfrac{1}{2}\Gamma_j(\tau_1 - \tau_2)]. \tag{12}$$

$|\psi_e(\tau)\rangle$ is the excited state part of the molecular wave function [the time-dependent version of Eq. (4)];

$$|\psi(\tau)\rangle = |g\rangle + |\psi_e(\tau)\rangle. \tag{13}$$

The physical picture of Eqs. (8)–(10) is as follows (Fig. 2.)[17b]: As the molecule is excited, the doorway state $|N_g\rangle$ is created. It then evolves in time. The emission into $|g'\rangle$ is governed by the projection of its doorway state $|N_{g'}\rangle$ onto the excited state wave function, given by Eq. (12).

Equation (8) is very general and corresponds to infinite temporal and frequency resolution in the detection. We shall consider now a simpler quantity with a finite frequency resolution which corresponds more realistically to experiment and is easier to calculate; namely, the time-dependent total photon emission rate into a final state $|g'\rangle$. This corresponds to an infinite time resolution but only moderate frequency resolution (we do not attempt to resolve the frequency profile in detail apart from specifying the final state $|g'\rangle$). This implies that the final photon frequency is $\omega_s \cong \omega_L - \omega_{gg'}$ with an uncertainty of the order of the excitation pulse bandwidth [see Eq. (16)]. Upon substituting Eq. (9) in Eq. (8) and integrating over ω_s we get

$$I_{g'}(t) = |\langle N_{g'}|\psi_e(t)\rangle|^2, \tag{14}$$

where $\langle N_{g'}|\psi_e(t)\rangle$ is the projection of the final doorway state $|N_{g'}\rangle$ onto the excited state wave function [Eq. (10)]. Hereafter we shall consider an ideal experiment in which $\phi(\tau)$ is very short; $\phi(\tau) \sim \delta(\tau)$. We then get

$$|\psi_e(t)\rangle = |N_g(t)\rangle \tag{15a}$$

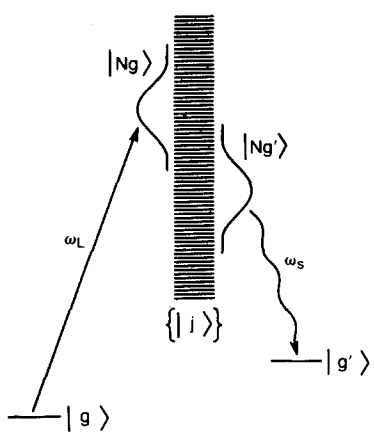

FIG. 2. The doorway state picture of fluorescence.[17(b)] $|N_g\rangle$ and $|N_{g'}\rangle$ are the doorway states corresponding to the initial ($|g\rangle$) and final ($|g'\rangle$) states, respectively. Their time-dependent overlap determines the time- and frequency-resolved fluorescence spectrum [Eqs. (8)–(10)].

so that

$$I_{g'}(t) = |\langle N_{g'}|N_g(t)\rangle|^2 = \sum_{jj'} |\mu_{gj}|^2|\mu_{g'j}|^2 \exp[-i\omega_{jj'}t - \tfrac{1}{2}(\Gamma_j + \Gamma_{j'})t]. \tag{15b}$$

Equations (2), (5), and (15) form the basis for our discussion in the next section.

III. DIRECT VERSUS REDISTRIBUTED FLUORESCENCE SPECTRA

We shall consider now a simplified model for the molecular level scheme which will enable us to distinguish between direct and redistributed components of the emission. It is clear from Eqs. (5) that in a frequency-resolved experiment, the only $|j\rangle$ states which are appreciably excited are those with $\omega_{jg} \cong \omega_L \pm \Gamma_j$. In a pulsed experiment the situation is slightly different. Suppose we measure the total number of photons emitted at each frequency ω_s, without attempting to resolve them in time. Upon integrating Eq. (8) over time we get (Appendix):

$$\langle I(\omega_L, \omega_s)\rangle = \int I(\omega_L + \omega, \omega_s)J(\omega)d\omega. \tag{16}$$

The number of ω_s photons is simply given by the steady state rate $I(\omega_L, \omega_s)$ [Eq. (5)] averaged over the power spectrum of the pulse. This shows that in a pulsed experiment the relevant $|j\rangle$ states are given by states in the vicinity of $\omega_{jg} \equiv \omega_L \pm (\Gamma_j + B)$ where B is the spectral bandwidth of the exciting pulse (of the order of a few wave numbers for good picosecond pulses). We shall denote the number of relevant $|j\rangle$ states by N. We shall further assume that the molecular modes may be classified into a few optically active "system" modes which are affected significantly by the optical transition, and many "bath" modes which are basically the same in both electronic states apart from a small (few percent) frequency shift.[2,17b] The allowed optical transitions are therefore those where the system quantum number may change $\Delta v_s = 0, 1, \ldots$, whereas the bath modes are restricted to diagonal transitions $\Delta v_B = 0$. These selection rules will determine the spectrum and are the reason for the usefulness of the harmonic basis for the description of these spectra. The state $|s\rangle$ which is the only zero-order state carrying oscillator strength from $|g\rangle$ in the energy region of interest is thus characterized by some value for v_s but has all $v_B = 0$ (since in the ground state $|g\rangle$ all $v_B = 0$). For simplicity we shall also neglect the anharmonicities in the ground state. (A brief discussion of their effect is given in the next section.) Under these conditions, the final states $|g'\rangle$ can be divided into two groups: Those with $v_B = 0$ which are accessible directly from the initial doorway state $|s\rangle$ and those with $v_B \neq 0$ which are accessible only from the $\{|l\rangle\}$ manifold. We shall denote these transitions as direct and redistributed spectra, respectively. It should be emphasized, however, that although the redistributed spectrum arises from the anharmonicities, it does not necessarily reflect a dynamical redistribution process. This will be discussed in detail shortly. It is clear that the former transitions will form a relatively simple

progression of lines, whereas the latter, by virtue of the large number of bath modes, and the frequency change in the optical excitation will form a complicated spectrum with many more lines. In the following discussion we shall distinguish only between these two groups. Further classification of the $\{|l\rangle\}$ transitions may of course be possible depending on the details of the molecular structure. (The $\{|l\rangle\}$ states may be separated into two or more manifolds with sequential couplings.[17]) Since our main purpose is to define the direct and the redistributed components and their frequency and time profiles, we shall not go further into the secondary classification of the $\{|l\rangle\}$ states. We shall now write explicit expressions for the experimental observables of Sec. II for this model showing the direct and the redistributed components and discuss the various possible cases.

(i) The absorption spectrum for the model is obtained using Eqs. (1) and (2):

$$I_a(\omega_L) = \sum_j |\alpha_j|^2 \delta(\omega_{jg} - \omega_L). \tag{17}$$

It reflects the mixing of $|s\rangle$ among the various molecular eigenstates $|j\rangle$.

(ii) The frequency-resolved emission. Upon substituting Eq. (1) in Eq. (5) we get

$$I(\omega_L, \omega_s) \equiv I_D + I_R, \tag{18}$$

$$I_D(\omega_L, \omega_s) = \sum_{g'} |\mu_{g's}|^2 \left| \sum_j \frac{|\alpha_j|^2}{\omega_{gj} - \omega_L + (i/2)\Gamma_j} \right|^2 \times \delta|\omega_{gg'} + \omega_L - \omega_s), \tag{18a}$$

$$I_R(\omega_L, \omega_s) \equiv \sum_l I_{R,l}, \tag{18b}$$

and

$$I_{R,l}(\omega_L, \omega_s) = \sum_{g'} |\mu_{g'l}|^2 \left| \sum_j \frac{\beta_{jl}\alpha_j}{\omega_{gj} - \omega_L + (i/2)\Gamma_j} \right|^2 \times \delta(\omega_{gg'} + \omega_L - \omega_s), \tag{18c}$$

where we have separated I into the direct component I_D and the redistributed emission from the $|l\rangle$ state $I_{R,l}$. I_D in general contains a relatively limited number of lines corresponding to progressions of the optically active system modes [i.e., few $|g'\rangle$ states will contribute to the sum (18a)]. I_R, however, is quite different. Due to the large number of the bath modes, $\omega_{gg'}$ will contain many lines and I_R will be very dense. We shall introduce now the *yield* Y of the direct component, i.e., the number of photons emitted in the direct component divided by the total number of emitted photons. To that end we define the integrated direct emission:

$$I_D(\omega_L) = \int I_D(\omega_L, \omega_s) d\omega_s = \left| \sum_j \frac{|\alpha_j|^2}{\omega_{gj} + \omega_L + (i/2)\Gamma_j} \right|^2, \tag{19a}$$

and the integrated total emission (which is identical with the absorption):

$$I_a(\omega_L) = I_D(\omega_L) + \sum_l \int I_{R,l}(\omega_L, \omega_s) d\omega_s = \sum_j \left| \frac{\alpha_j}{\omega_{gj} + \omega_L + (i/2)\Gamma_j} \right|^2. \tag{19b}$$

(We assume a unit oscillator strength $\left(\sum_{g'} |\mu_{sg'}|^2 = \sum_{g'} \times |\mu_{lg'}|^2 = 1. \right)$ In a frequency-resolved experiment the direct yield, therefore, will be

$$Y \equiv I_D(\omega_L)/I_a(\omega_L) = \left| \sum_j \frac{|\alpha_j|^2}{\omega_{gj} + \omega_L + (i/2)\Gamma_j} \right|^2 \Bigg/ \sum_j \left| \frac{\alpha_j}{\omega_{gj} + \omega_L + (i/2)\Gamma_j} \right|^2. \tag{19c}$$

Using Eq. (16) we get for a pulsed experiment

$$Y = \int d\omega\, I_D(\omega_L + \omega) J(\omega) \Big/ \int d\omega\, I_a(\omega_L + \omega) J(\omega). \tag{20}$$

Equations (19) and (20) express the yield in terms of the exact molecular eigenstates $\{|j\rangle\}$.

An alternative expression for I_a, I_D and the yield in terms of the zero-order (harmonic) basis set $|s\rangle$, $\{|l\rangle\}$ may be derived using the Green's function.[17b]

$$G_{ss}(\omega_L) \equiv \left\langle s \left| \frac{1}{E_g + \omega_L - H} \right| s \right\rangle. \tag{21}$$

Eqs. (19) may then be written in the form

$$I_a(\omega_L) = (-2/\gamma)\ \mathrm{Im}\ G_{ss}(\omega_L), \tag{22a}$$

and

$$I_D(\omega_L) = |G_{ss}(\omega_L)|^2, \tag{22b}$$

so that

$$Y = \frac{-\gamma |G_{ss}(\omega_L)|^2}{2\ \mathrm{Im}\ G_{ss}(\omega_L)}. \tag{23}$$

Here γ is the radiative width of the states $|s\rangle$ and $\{|l\rangle\}$.

The Green's function G_{ss} may further be written in the form

$$G_{ss}(\omega_L) = \frac{1}{E_g + \omega_L - E_s - \Delta_s(\omega_L) + (i/2)[\Gamma_s(\omega_L) + \gamma]}. \tag{24}$$

Here Δ_s and Γ_s are the real and imaginary parts, respectively, of the self-energy operator:

$$\Delta_s(\omega_L) - \frac{i}{2}\Gamma_s(\omega_L) = \sum_l \frac{|V_{sl}|^2}{\omega_{gl} + \omega_L + (i/2)\gamma}, \tag{25}$$

that is,

$$\Delta_s(\omega_L) = \sum_l \frac{|V_{sl}|^2(\omega_{gl} + \omega_L)}{(\omega_{lg} - \omega_L)^2 + \frac{1}{4}\gamma^2}, \tag{25a}$$

and

$$\Gamma_s(\omega_L) = \sum_l \frac{|V_{sl}|^2\gamma}{(\omega_{lg} - \omega_L)^2 + \frac{1}{4}\gamma^2}. \tag{25b}$$

Upon the substitution of Eq. (24) in Eq. (23) we finally get

$$Y = \frac{\gamma}{\gamma + \Gamma_s(\omega_L)}. \tag{26}$$

Equation (26), together with Eq. (25b), provide a convenient expression for the yield in terms of the zero-order coupling parameters, which is more convenient to use than Eq. (19c) since it does not require the calculation of the exact molecular eigenstates $|j\rangle$. If the manifold $\{|l\rangle\}$ is sufficiently dense, such that the level spacings are smaller than γ, it becomes an effective continuum, and in that case $\Gamma_s(\omega_L)$ becomes a constant independent on ω_L. Equation (26) then corresponds to a simple kinetic scheme, whereby the excited state has two parallel channels for decay: a direct emission with rate γ, and a redistribution process with a rate Γ_s [see Eq. (45)]. In general, however, Γ_s will be a strongly oscillatory function of ω_L, and this oscillatory structure will be reflected in the yield. Moreover, for large off-resonance detunings, when $|\omega_{lg} - \omega_L|$ is much larger than γ for any $|l\rangle$, it is clear from Eq. (25b) that $\Gamma_s(\omega_L)$ will then eventually vanish, i.e., for large detunings.

$$\Gamma_s(\omega_L) \sim (\omega_{sg} - \omega_L)^{-2} \to 0, \tag{27a}$$

so that

$$Y(\omega_L) \to 1, \tag{27b}$$

i.e., the yield Y will always go to 1 for large detunings. The reason is that the emission process for large detunings is very fast, and the $|s\rangle$ doorway state does not have time to evolve, resulting in a purely direct (unredistributed) emission. Fluorescence at large detunings (i.e., Raman spectra) may thus provide information regarding the short-time emission, similar to what is obtained from time- and frequency-resolved experiments or from chemical timing techniques. The short-time or large detuning spectra will always be simple and unredistributed. Another way to see that is from Eq. (4), which shows that for a resonance detuning, $|\psi_e\rangle$ contains a few selected $|j\rangle$ states. However, as the detuning increases, the denominator in Eq. (4) becomes constant (i.e., insensitive to ω_{gj}), and $|\psi_e\rangle$ turns gradually into $|s\rangle$.

This result reflects the well-known fact that Raman spectra which are performed at large detunings are not sensitive to the excited state dynamics and provide mainly ground state information.[23,24] The disappearance of the redistributed component in collisional broadening of Raman spectra at large detunings is another manifestation of the same effect.[23]

(iii) Time and frequency resolved spectra. We consider an ideal pulsed experiment whereby the excitation pulse is short compared with the frequency spread $\omega_{jj'}$ of an isolated group of molecular eigenstates. The (normalized) initial wave packet following the excitation is thus

$$|\psi_e(0)\rangle = \frac{1}{\sqrt{\sum_j |\alpha_j|^2}} \sum_j \alpha_j^* |j\rangle. \tag{28}$$

The direct component will then be

$$I_D(t) = \gamma P_s(t) = \gamma|\langle s|\psi_e(t)\rangle|^2. \tag{29}$$

Assuming the radiative widths (γ) to be the same for all $|j\rangle$ states we get

$$I_D(t) = \gamma\chi(t)\exp(-\gamma t), \tag{30a}$$

and

$$I_R(t) = \gamma[1 - \chi(t)]\exp(-\gamma t), \tag{30b}$$

where

$$\chi(t) = \frac{1}{\sum_j |\alpha_j|^2}\left|\sum_j |\alpha_j|^2 \exp(-iE_j t - \tfrac{1}{2}\Gamma_j t)\right|^2, \tag{30c}$$

where Γ_j now denotes the nonradiative width of $|j\rangle$. Note that we have normalized I_D and I_R such that

$$\int_0^\infty I_D(\tau)d\tau + \int_0^\infty I_R(\tau)d\tau = 1. \tag{31}$$

We can introduce a time dependent yield $Y(t)$ giving the fraction of "direct" photons emitted at time t, i.e.,

$$Y(t) \equiv I_D(t)/[I_D(t) + I_R(t)] = \chi(t). \tag{32}$$

The integrated yield (over time) is given by

$$Y = \int_0^\infty d\tau\, I_D(\tau) = \frac{\gamma}{\sum_j |\alpha_j|^2} \sum_{j \geqslant j'} |\alpha_j|^2|\alpha_{j'}|^2 \frac{\hat{\Gamma}_{jj'}}{\omega_{jj'}^2 + \hat{\Gamma}_{jj'}^2}, \tag{33}$$

where

$$\hat{\Gamma}_{jj'} \equiv \tfrac{1}{2}(\Gamma_j + \Gamma_{j'}) + \gamma. \tag{33a}$$

Equations (17), (19), (26), and (30)–(33) are the main results of this section. We are now in a position to discuss the various cases and the experimental distinction between the direct and the redistributed components. Since the temporal behavior is mainly governed by the number N of relevant $|j\rangle$ states, we shall classify the various cases according to this criterion.

A. Case A: Only one relevant eigenstate $|j\rangle$ ($N = 1$)

When a single eigenstate $|j\rangle$, well separated from its neighbors, can be identified so that its distance from its nearest neighbor $\omega_{jj'}$ is much larger than their widths $\Gamma_j + \Gamma_{j'}$, the laser detuning $\omega_{gj} + \omega_L$, and the laser bandwidth B, then that particular $|j\rangle$ will be dominant in Eqs. (18) and (28) and to a good approximation we can ignore the contributions of all other states $|j\rangle$. In this case there is no intramolecular vibrational dynamics in the experiment. In an ideal time-resolved (short excitation) experiment we simply have

$$|\psi_e(t)\rangle = \exp[-iE_j t - \tfrac{1}{2}(\Gamma_j + \gamma)t]|j\rangle, \tag{34a}$$

$$|\langle s|\psi_e(t)\rangle|^2 = |\alpha_j|^2, \tag{34b}$$

so that in Eq. (30) $\chi(t) = |\alpha_j|^2$, i.e.,

$$I_D(t) = |\alpha_j|^2 \exp(-\gamma t), \tag{35a}$$

$$I_R(t) = [1 - |\alpha_j|^2]\exp[-\gamma t]. \tag{35b}$$

The doorway state contains an $|\alpha_j|^2$ fraction of $|s\rangle$ character and $1 - |\alpha_j|^2$ redistributed character. The time evolution of I_D and I_R is only radiative and is identical. The yield

$$Y = |\alpha_j|^2, \tag{36}$$

merely reflects a *static mixing,* carries no dynamical information, and is the same for a frequency-resolved and for a pulsed experiment. The experimental characteristics in this case are, therefore, as follows: The absorption is given by a well-resolved single line $\delta(\omega_L - \omega_{jg})$, there is no vibrational dynamics in the experiment, and the doorway state $|j\rangle$ simply decays radiatively. The frequency-resolved emission spectrum [Eq. (18)] may be, however, either very simple (when $\alpha_j \sim 1$) or very rich and "redistributed" (when $\alpha_j \sim 0$) reflecting the nature of $|j\rangle$. *Neither the appearance of the redistributed component, nor its shape, nor yield contain any dynamical information in this case.*[15]

B. Case B: The intermediate case, few relevant $|j\rangle$ states

In this case the doorway state undergoes nontrivial vibrational dynamics. The spectrum will contain quantum beats resulting from transfer of energy back and forth among the harmonic vibrational states [Eq. (30)]. Note that the observability of quantum beats depends on the frequency resolution in the experiment. If we just measure the total time-resolved emission with no frequency resolution at all, then from Eq. (30) we get

$$I(t) \equiv I_D(t) + I_R(t) = \gamma \exp(-\gamma t), \tag{37}$$

and we lose all the information regarding IVR contained in $\chi(t)$.

On the other hand, with a too good frequency resolution we may also lose the beats. If we resolve the emission from each $|j\rangle$ state we simply get a signal proportional to

$$P_j(t) = P_j(0)\exp[-(\Gamma_j + \gamma)t], \tag{38}$$

which again contains no IVR information. The quantum beats will be observed only if we have a *mixed excitation* whereby several $|j\rangle$ states are coherently excited, followed by a moderately resolved detection in which we detect emission to a given $|g'\rangle$ level. If the initial excitation selects one $|j\rangle$ (case A) we do not observe IVR since it does not exist. If the final doorway state $|N_{g'}\rangle$ projects only on one $|j\rangle$ state we shall not observe IVR even if it occurs since the experiment is "too good" and resolves individual eigenstates $|j\rangle$. *Only at intermediate frequency resolution will the quantum beats be observed.* The importance of a combined frequency and time resolution for the detection of quantum beats was clearly demonstrated by the works of Zewail, Parmenter, and coworkers.[2,16]

Let us turn now to the yield of the direct emission. At $t = 0$ it is [Eq. (32)]

$$Y(t = 0) = \sum_j |\alpha_j|^2 \tag{39}$$

which merely reflects the "$|s\rangle$" character of the initially prepared doorway state. The total (integrated) yield [Eq. (33)] is

$$Y = \sum_j |\alpha_j|^4 \Big/ \sum_j |\alpha_j|^2 + \sum_{j>j'} \frac{\hat{\Gamma}_{jj'}^2}{\omega_{jj'}^2 + \hat{\Gamma}_{jj'}^2} |\alpha_j|^2|\alpha_{j'}|^2 \Big/ \sum_j |\alpha_j|^2. \tag{40}$$

We note two limiting cases for Y [Eq. (40)]. When the levels $|j\rangle$ are much closer than their widths $\omega_{jj'} \ll \hat{\Gamma}_{jj'}$ we have

$$Y = \sum_j |\alpha_j|^2, \tag{41a}$$

whereas in the opposite limit, when the levels are well separated $\omega_{jj'} \gg \hat{\Gamma}_{jj'}$ we get

$$Y = \sum_j |\alpha_j|^4 \Big/ \sum_j |\alpha_j|^2. \tag{41b}$$

It is clear that Eq. (41a) is an upper bound for the yield, whereas Eq. (41b) is a lower bound and the actual yield [Eq. (40)] always lies between these values. In case A there is no dynamics and the yield is independent on time so that Eq. (41a) coincides with $Y(t = 0)$ [Eq. (39)]. When dynamics takes place, Y will always be smaller than the yield at $t = 0$ [Eq. (41a)] since a certain fraction of the intensity will be redistributed. The difference between Y [Eq. (40)] and $Y(t = 0)$ [Eq. (39)] thus reflects the dynamical effect of IVR.

Y^{-1} [Eq. (41b)] is known in the theory of the Anderson localization as the "participation ratio"[25] and was introduced as a measure of how localized is the wave function for a motion in a random potential or how local are the vibrational modes of a disordered solid. Y^{-1} measures roughly the number N of levels among which $|s\rangle$ is spread. If all α_j are equal then $Y^{-1} = N$. More precisely, using Eqs. (29) and (33) we see that Y actually measures the fraction of time the excited state $|\psi_e\rangle$ [Eq. (28)] spends in the $|s\rangle$ state. The value $Y^{-1} = N$ is a "democratic" estimate of that fraction. The participation ratio [Eq. (41b)] appeared naturally in the discussion of the short and long components in radiationless transitions[17,26,27] [see Eq. (43a)] and was discussed again recently.[28]

C. Case C: The statistical limit

When $\Gamma_j = 0$ (the $|j\rangle$ states contain no nonradiative width), Eq. (30a) may be recast in the form[26,27]

$$I_D(t) = \frac{\gamma}{\sum_j |\alpha_j|^2}\left\{\sum_{j\neq j'=1}^{N} |\alpha_j|^2|\alpha_{j'}|^2 \exp[-i\omega_{jj'}t - \gamma t] + \sum_{j=1}^{N} |\alpha_j|^4 \exp(-\gamma t)\right\}. \quad (42)$$

The first term will decay faster than the second due to the dephasing of the $\exp(-i\omega_{jj'}t)$ term. For large enough N, Eq. (42) may look like a biexponential decay

$$I_D(t) = A_+ \exp[-(\Gamma + \gamma)t] + A_- \exp(-\gamma t), \quad (43)$$

where Γ is the dephasing width and

$$A_+/A_- \sim N. \quad (43a)$$

In the statistical limit the manifold $\{|l\rangle\}$ is very dense and consequently $N \gg 1$. Under these conditions the first term in Eq. (43) becomes dominant and we get

$$I_D(t) = \gamma \exp[-(\Gamma + \gamma)t], \quad (44a)$$

$$I_R(t) = \gamma[1 - \exp(-\Gamma t)]\exp(-\gamma t), \quad (44b)$$

where

$$\Gamma = 2\pi|V_{sl}|^2\rho_l, \quad (44c)$$

being the inverse lifetime of $|s\rangle$. Here ρ_l is the density of states in the $\{|l\rangle\}$ manifold. In this case, the yield [Eq. (33)] becomes

$$Y = \gamma/(\Gamma + \gamma), \quad (45)$$

as may be expected from a simple kinetic scheme. Another way to see this limit is by using Eq. (26). In the statistical limit Γ_s becomes simply independent on frequency (the Markovian limit) and Eq. (26) reduces to Eq. (45). Let us see how this limit is obtained from Eq. (33). Assuming an equally spaced manifold with constant coupling V_{sl} we have[29]

$$\alpha_j = \frac{1}{\sqrt{\pi}} \frac{\sqrt{\gamma}}{\epsilon_j + (i/2)\gamma} \rho_l^{-1/2} \quad (46)$$

and

$$\epsilon_j = \rho_l^{-1} j.$$

Upon switching the summation in Eq. (33) to integration $\sum_j \to \int \rho d\epsilon_j$ we get

$$Y = \gamma \int\int d\epsilon\, d\epsilon' \frac{1}{\pi^2} \frac{\gamma}{\epsilon^2 + (1/4)\gamma^2} \frac{\gamma}{\epsilon'^2 + (1/4)\gamma^2} \times \frac{\Gamma}{(\epsilon - \epsilon')^2 + \Gamma^2} = \frac{\gamma}{\Gamma + \gamma}. \quad (47)$$

In this limit, information regarding the individual eigenstate is lost and the interpretation of Y is purely dynamical. Note also that in the statistical limit $Y(t = 0) = 1$. That is, initially we prepare the $|s\rangle$ state which then decays, resulting in the smaller yield [Eq. (47)].

IV. DISCUSSION

One of the key issues in the fluorescence studies of supercooled polyatomic molecules is to what extent they contain dynamic information regarding IVR processes. The reason for conducting these studies on ultracold molecules in supersonic beams is to eliminate various sources of inhomogeneous (static) line broadening (sequences, rotational envelopes, etc.) which otherwise dominate these spectra and prevent us from addressing the problems of intramolecular dynamics. Time- and frequency-resolved experiments are capable of addressing these questions directly by monitoring the temporal profile of various parts of the emission spectrum following a pulsed excitation. The existence of different types of time evolution is a signature of the intramolecular dynamics as reflected in the time-dependent populations of the doorway states $|N_{g'}\rangle$. Experiments which are only frequency resolved address this issue indirectly and are thus usually inconclusive regarding their dynamical information. Anharmonicities have a static as well as dynamic effect on the molecular spectra and without a time-resolved detection it is virtually impossible to distinguish between the two. The nature of the intramolecular dynamics and the *time-resolved* fluorescence is mainly determined by the number N of relevant eigenstates which participate in the experiment. We have distinguished between case A ($N = 1$) where no dynamics is involved and the entire effect of anharmonicities is static, case B where N is small and the spectra contain both static and dynamic features, and finally case C where N is very large and the observables contain purely dynamical information. The complexity of the *frequency-resolved* spectra depends, on the other hand, on the number M of harmonic states $\{|l\rangle\}$ which are significantly coupled to $|s\rangle$. This will determine the number of different $|g'\rangle$ states contributing to Eq. (18c). *This number M is not necessarily related to N.* In case A, e.g., where $N = 1$, M can be either very small (simple emission spectrum) or very large. Felker and Zewail have recently observed all three cases in anthracene.[16] An intermediate case behavior was observed with an excitation vibrational energy of 1490 cm^{-1}. The following features were observed: (i) The emission exhibits a beat pattern corresponding to three eigenstates ($N = 3$). Both I_D and I_R were measured. (ii) The dispersed emission spectrum is quite complex implying that the number M of harmonic states participating in the spectrum is very large. (iii) The short time yield $Y(t = 0)$ [Eq. (39)] is 1 (i.e., only direct emission is observed initially, and the redistributed component builds up with time). One of the most important questions in the dynamics of highly vibrationally excited anharmonic molecules is whether the anharmonic coupling scheme is *statistical* and "democratic" (i.e., every harmonic state is roughly equally coupled to all the other harmonic states in its vicinity) or does it have specific propensity rules, whereby the coupling is highly *selective* and each harmonic state is coupled

only to relatively few states. We shall now discuss this issue for anthracene at ~ 1490 cm^{-1} of vibrational excitation, in the light of observations (i)–(iii). Observation (i) ($N = 3$) implies that the experiment selected three eigenstates which are well separated from the rest, and which carry $|s\rangle$ character. The complexity of the frequency-resolved emission [observation (ii)], however, suggests that these eigenstates are complicated mixtures of many harmonic states ($M \gg 1$), otherwise the emission will be simple and discrete. These two observations are compatible with both a statistical [Fig. 3(A)] and a selective [Fig. 3(B)] anharmonic coupling scheme. In Fig. 3(A), the doorway state is coupled to many harmonic states. In Fig. 3(B), it is coupled selectively only to two harmonic ($|l_1\rangle$ and $|l_2\rangle$) which are subsequently coupled to the rest. Both coupling schemes can lead to a situation in which $N = 3$ and $M \gg 1$, as implied by observations (i) and (ii). This simply means that we have three isolated eigenstates, each of which is a linear combination of many harmonic states. The short time yield $Y(t = 0)$ [observation (iii)] allows us, however, to distinguish between the schemes of Fig. 3(A) and Fig. 3(B). For a statistical coupling we expect the doorway state to be diluted among many ($M \gg 1$) eigenstates, so that each $|\alpha_j|^2$ is $\sim 1/M$. Since only three eigenstates participate ($N = 3$), then the sum over j in Eq. (39) goes over these three states, so that $Y(t = 0) \sim 3/M \ll 1$. The spectrum at $t = 0$ will be mainly redistributed, and superimposed on it will be a small beat pattern, phase shifted with respect to the direct component. Let us turn, on the other hand, to scheme B. We can first prediagonalize the $\{|l\rangle\}$ manifold, transforming Fig. 3(B) into Fig. 3(C), where $|s\rangle$ is coupled to two states $|\tilde{l}\rangle$, each being a complicated superposition of many harmonic states. In this case, $|s\rangle$ is spread only among three eigenstates, $|\alpha_j|^2 \sim 1/3$ and $Y(t = 0) \sim 1$. The emission at $t = 0$ is *direct,* and the redistributed component builds up as time progresses. This behavior is compatible with observation (iii). Another way to see this is by noting that observation (i) indicates that the initially prepared state is a superposition of three eigenstates. If $|s\rangle$ is spread among M states ($M \gg 1$), then the probability of the molecule to be initially in the $|s\rangle$ state is $3/M$, and the initial emission will be mainly redistributed. However, if $|s\rangle$ is spread only among these three states, then the initial wave packet will be exactly $|s\rangle$, and the initial emission will be purely "direct." We thus conclude that the appearance of a simple time resolved pattern ($N = 3$), with $Y(t = 0) = 1$, and with a complicated emission spectrum is compatible with the selective coupling scheme [Fig. 3(B)]. A similar conclusion was obtained by McDonald and co-workers in their studies of infrared fluorescence in dimethyl ether[30] and by Parmenter *et al.,* in their chemical timing spectroscopy.[2]

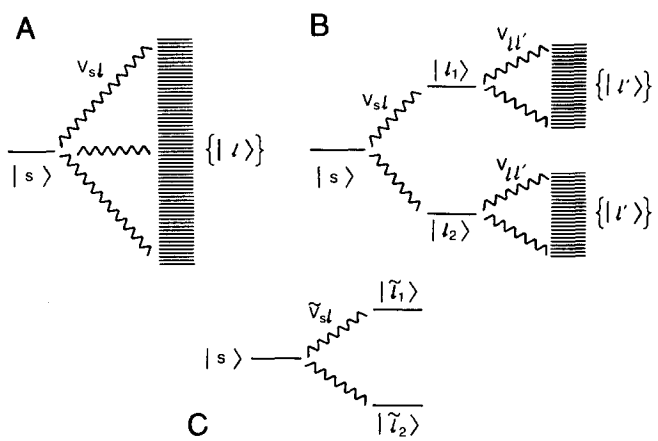

FIG. 3. "Democratic" vs "sequential" anharmonic coupling schemes. $|s\rangle$ and $\{|l\rangle\}$ are harmonic states. By prediagonalizing the $\{|l\rangle\}$ manifold, we may transform the level scheme of (B) into (C).

In conclusion, we should note the following: the obvious criterion to whether the fluorescence carries any dynamical information is whether different parts of the emission spectrum exhibit a different time evolution. While the existence of such variation is a proof for IVR, its absence is not conclusive. As was shown in our discussion on quantum beats (case B), it could be that the detection resolution is too good or too poor for the observation of IVR. Also, the IVR could occur on a faster time scale than the experimental resolution. Our analysis shows that the interpretation of fluorescence spectra, which are only frequency resolved, is usually ambiguous, and it is difficult to extract from them direct dynamical information. When both direct and redistributed components may be frequency resolved, it is tempting to assume that case C applies, and that simple rate equations may be used. As a result, the integrated ratio of the direct and redistributed components yields the IVR rate Γ via Eq. (45), if the radiative lifetime γ is known. We have shown that for alkyl benzenes this is not the case.[14,15] Time-resolved (nanosecond) experiments showed that the IVR rate so extracted is not correct since these molecules at ~ 2000 cm^{-1} of vibrational energy belong to case A or B. A similar procedure was applied recently[31] for the calculation of an intramolecular electronic energy transfer rate by assuming that case C holds. This assumption must be verified by frequency- and time-resolved measurements before accepting the rate obtained this way.

In principle, a highly resolved absorption (excitation) spectrum should reveal the number N of $|j\rangle$ levels, thus yielding the same information contained in the quantum beats. In real life, however, the absorption is often dominated by a residual inhomogeneous broadening (sequences, rotations) which obscures this information. In addition, if the widths Γ_j are comparable to the spacings $\omega_{jj'}$ the spectrum becomes difficult to interpret. Therefore time- and frequency-resolved experiments are usually much more informative than merely frequency-resolved experiments. It should be noted that anharmonicities in the ground state will obscure the distinction between the direct and the redistributed spectra. The state $|g'\rangle$ will be a mixture of "system" and "bath" types of states, and the two types of emission may become indistinguishable. Another point which should be mentioned is that in the statistical limit when the $\{|l\rangle\}$ states can be divided into several groups with distinct spectral features, the simplest description of the fluorescence is given by a master

equation. Some experimental data on the tetrazine–argon complex[31,32] suggest that this may be the case, although it is not clear at the moment whether those experiments are collision free. A complete derivation and discussion of the application of master equations to fluorescence in molecules with IVR was made recently[15] and is analogous to the treatment of fluorescence in macroscopic systems.[23]

ACKNOWLEDGMENTS

I wish to thank the kind hospitality of A. Tramer and the Laboratoire de photophysique Moleculaire (Orsay) where this work was completed. Stimulating discussions with A. Tramer, A. H. Zewail, J. Kommandeur, and R. Rettschnick are most appreciated. The support of the National Science Foundation and the Petroleum Research Fund administered by the American Chemical Society is gratefully acknowledged.

APPENDIX: THE TIME INTEGRATED YIELD FOR A PULSED EXCITATION

Equations (9) and (10) can be written using a Fourier transform:

$$C_{g'g}(t) = (1/2\pi i)\int_{-\infty}^{\infty} dE\, \exp(-iEt) C_{g'g}(E), \tag{A1}$$

where

$$C_{g'g}(E) = \frac{1}{E - \omega_s - E_{g'}} G_{N'N}(E)\phi(E - E_g - \omega_L), \tag{A2}$$

where $\phi(E)$ is given by Eq. (7c), and

$$G_{N'N}(E) \equiv \langle N_{g'}| \frac{1}{E - H} |N_g\rangle. \tag{A3}$$

Equations (A1) and (A2) result in

$$\begin{aligned}|C_{g'g}(t)|^2 &= \int_{-\infty}^{\infty} dE \int_{-\infty}^{\infty} dE' \exp[-i(E' - E)t]\phi(E - E_g - \omega_L) \\ &\times \phi^*(E' - E_g - \omega_L) \times G_{N'N}(E) G^*_{N'N}(E') \\ &\times \left[\frac{1}{E - \omega_s - E_{g'}} - \frac{1}{E' - \omega_s - E_{g'}}\right] \frac{1}{E' - E}. \end{aligned} \tag{A4}$$

Upon the substitution of Eq. (A4) in Eq. (8) we get

$$\begin{aligned} I_g(\omega_L, \omega_s, t) &\equiv \frac{d}{dt} |C_{g'g}(t)|^2 \\ &= \int_{-\infty}^{\infty} dE \int_{-\infty}^{\infty} dE' \exp[-i(E' - E)t] \times \phi(E) \\ &\times \phi^*(E') G_{N'N}(E + E_g + \omega_L) \\ &\times G^*_{N'N}(E' + E_g + \omega_L) \left[\frac{1}{E + \omega_{gg'} + \omega_L - \omega_s} \right. \\ &\left. - \frac{1}{E' + \omega_{gg'} + \omega_L - \omega_s}\right]. \end{aligned} \tag{A5}$$

Upon integrating Eq. (A5) over time we get

$$\begin{aligned} \langle I(\omega_L, \omega_s)\rangle &\equiv \int_{-\infty}^{\infty} dt \sum_{g'} I_{g'}(\omega_L, \omega_s, t) \\ &= \sum_{g'} \int_{-\infty}^{\infty} dE |\phi(E)|^2 |G_{N'N}(E + E_g + \omega_L)|^2 \\ &\times \delta(E + \omega_{gg'} + \omega_L - \omega_s) \\ &\equiv \int_{-\infty}^{\infty} d\omega\, J(\omega) I(\omega_L + \omega, \omega_s), \end{aligned} \tag{A6}$$

where we have used the definitions Eqs. (5) and (7b). This proves Eq. (16).

[1] D. H. Levy, L. Wharton, and R. E. Smalley in *Chemical and Biochemical Applications of Lasers,* edited by C. B. Moore (Academic, New York, 1977) Vol. II; R. R. Langridge-Smith, D. V. Brumbaugh, C. A. Hoynam, and D. H. Levy, J. Phys. Chem. **85,** 3742 (1981); D. H. Levy, Annu. Rev. Phys. Chem. **31,** 197 (1980).
[2] C. S. Parmenter, J. Phys. Chem. **86,** 1735 (1982).
[3] R. E. Smalley, J. Phys. Chem. **86,** 3504 (1982); Annu. Rev. Phys. Chem. **34,** 129 (1983).
[4] A. Amirav, U. Even, and J. Jortner, J. Phys. Chem. **86,** 3345 (1982); J. Chem. Phys. **75,** 3770 (1981).
[5] V. E. Bondybey, Annu. Rev. Phys. Chem. **35,** 591 (1984).
[6] E. Riedle, H. J. Neusser, and E. W. Schlag, J. Phys. Chem. **86,** 4847 (1982); H. Henke, H. L. Selzle, T. R. Hays, S. H. Lin, and E. W. Schlag, Chem. Phys. Lett. **77,** 448 (1981).
[7] B. J. Van Der Meer, H. Th. Jonkman, J. Kommandeur, W. L. Meerts, and W. A. Majewski, Chem. Phys. Lett. **92,** 565 (1982); J. Kommandeur, Recl. J. Roy. Neth. Chem. Soc. **102,** 421 (1983).
[8] C. Bouzou, C. Jouvet, J. B. Lebond, Ph. Millie, A. Tramer, and M. Sulkes, Chem. Phys. Lett. **97,** 181 (1983); B. Fourmann, C. Jouvet, A. Tramer, J. M. LeBars, and Ph. Millie, Chem. Phys. **92,** 25 (1985).
[9] W. R. Lambert, P. M. Felker, and A. H. Zewail, J. Chem. Phys. **75,** 5958 (1981); P. M. Felker and A. H. Zewail, Chem. Phys. Lett. **102,** 113 (1983).
[10] J. Chaiken, M. Gurnick, and J. M. McDonald, J. Chem. Phys. **75,** 106 (1981).
[11] S. Okajima, H. Sarbusa, and E. C. Lim, J. Chem. Phys. **76,** 2096 (1982).
[12] P. H. Vaccaro, J. L. Kinsey, R. W. Field, and H. L. Dai, J. Chem. Phys. **78,** 3659 (1983).
[13] A. Amirav, U. Even, and J. Jortner, J. Chem. Phys. **71,** 2319 (1979); U. Even, Y. Magen, J. Jortner, and H. Levanon, J. Am. Chem. Soc. **103,** 4583 (1981); J. Chem. Phys. **76,** 5684 (1982); U. Even and J. Jortner, *ibid.* **77,** 4391 (1982).
[14] J. B. Hopkins, D. E. Powers, S. Mukamel, and R. E. Smalley, J. Chem. Phys. **72,** 5049 (1980).
[15] S. Mukamel and R. E. Smalley, J. Chem. Phys. **73,** 4156 (1980).
[16] P. M. Felker and A. H. Zewail, Phys. Rev. Lett. **53,** 501 (1984); Chem. Phys. Lett. **108,** 303 (1984); W. R. Lambert, P. M. Felker, and A. H. Zewail, J. Chem. Phys. **81,** 2209 (1984); **81,** 2217 (1984).
[17] (a) J. Jortner and S. Mukamel, in *The World of Quantum Chemistry,* edited by R. Daudel and R. Pullman (Reidel, Dordrecht, 1973) p. 145; J. Jortner and S. Mukamel in *Theoretical Chemistry,* edited by A. D. Buckingham (Butterworths, London, 1975), MTP Ser. 2, Vol. 1, p. 327; J. Jortner and S. Mukamel, in *Molecular Energy Transfer,*

edited by R. D. Levine and J. Jortner (Wiley, New York, 1976) p. 178; (b) S. Mukamel and J. Jortner, in *Excited States,* edited by E. C. Lim, (Academic, New York, 1977), Vol. 3, p. 57.
[18] S. H. Lin, *Radiationless Transitions,* (Academic, New York, 1980).
[19] K. F. Freed, Top. Appl. Phys. **15,** 23 (1976).
[20] A. Tramer and R. Voltz, in *Excited States,* edited by E. C. Lim (Academic, New York, 1979), Vol. 4, p. 281.
[21] A. Amirav, M. Sonnenschein, and J. Jortner, Chem. Phys. **88,** 199 (1984).
[22] It is, of course, impossible to have infinite temporal and spectral resolution, and a realistic detection device will introduce a certain uncertainty by averaging $I_g(\omega_L, \omega_s, t)$ over ω_s, or t, or both.
[23] S. Mukamel, Phys. Rep. **93,** 1 (1982).
[24] J. Tang and A. C. Albrecht, in *Raman Spectroscopy,* edited by H. A. Szymanski (Plenum, New York, 1970), Vol. 2, p. 33.
[25] R. J. Bell and P. Dean, Discuss. Faraday Soc. **50,** 55 (1970); D. J. Thouless, Phys. Rep. C **13,** 93 (1974).
[26] F. Lahmani, A. Tramer, and C. Tric, J. Chem. Phys. **60,** 4431 (1974); A. Frad, F. Lahmani, A. Tramer, and C. Tric, J. Chem. Phys. **60,** 4419 (1974).
[27] J. Kommandeur, B. J. Van Der Meer, and H. Th. Jonkman, in *Intramolecular Dynamics,* edited by J. Jortner and B. Pullman (Reidel, Dordrecht, 1982), p. 259; B. J. Van Der Meer, H. Th. Jonkman, and J. Kommandeur, Laser Chem. **2,** 77 (1983).
[28] M. J. Davis and E. J. Heller, J. Chem. Phys. **80,** 5036 (1984).
[29] U. Fano, Phys. Rev. **124,** 1866 (1961).
[30] G. Stewart, R. Ruoff, T. Kulp, and J. D. McDonald, J. Chem. Phys. **80,** 5353 (1984); **80,** 5359 (1984).
[31] T. Ebata, Y. Suzuki, N. Mikami, T. Miyashi, and M. Ito, Chem. Phys. Lett. **110,** 597 (1984).
[32] J. J. Ramaekers, H. M. Van Dijk, L. Langelaar, and R. P. H. Rettschnick, Faraday Discuss. Chem. Soc. **75** (1983); J. J. F. Ramaekers, Thesis, University of Amsterdam, 1983.